Applied Acoustics 183 (2021) 108325

Contents lists available at ScienceDirect

Applied Acoustics

journal homepage: www.elsevier.com/locate/apacoust

A sound based method for fault detection with statistical feature extraction in UAV motors

Ayhan Altinors [a,*], Ferhat Yol [a], Orhan Yaman [b]

[a] Department of Electronics and Automation, Vocational School of Technical Sciences, Firat University, Elazig, Turkey
[b] Department of Digital Forensics Engineering, Firat University, Elazig, Turkey

ARTICLE INFO

Article history:
Received 6 May 2021
Received in revised form 29 June 2021
Accepted 20 July 2021
Available online 28 July 2021

Keywords:
UAV motors
Statistical feature extraction
Machine learning
Sound-based fault detection

ABSTRACT

The motors of the Unmanned Aerial Vehicle are critical parts, especially when used in applications such as military and defense systems. The fact that the brushless DC (BLDC) motors used in UAVs operate at high speed causes malfunctions. In this study, propeller, eccentric and bearing failures, which are frequently seen in UAV motors, were created. Then the fault diagnosis was made by applying the recommended method on the sound data received from the motors. Signal pre-processing, feature extraction, and machine learning methods were applied to the obtained sound dataset. Decision tree (DT), Support Vector Machines (SVM), and k Nearest Neighbor (KNN) algorithms are used for machine learning. The results have been obtained using three different UAV motors of 1400 KV, 2200 KV, and 2700 KV. For the 2200 KV motor, the accuracy of 99.16%, 99.75%, and 99.75% was calculated in DT, SVM, and KNN algorithms, respectively. The high accuracy of the proposed method indicates that the study will contribute to the studies in the relevant field. Another advantage is that the method is fast and able to work in real-time on embedded systems.

1. Introduction

1.1. Background

Electric motors are widely used both in daily use and in industry. Especially in the defense industry, high-speed electric motors are used [1]. Different DC motors are preferred according to the characteristics of UAVs. Failure of electric motors creates problems such as the inability of UAVs to fulfill their duties. Thus, both the operation fails and causes major accidents.

2. Research motivation

Unmanned aerial vehicles are increasingly used for civilian and military purposes in many applications ranging from observation, search and rescue, target detection, combat, surveillance, environmental monitoring, disaster area research, and scientific mapping. Failure of UAVs when used mostly for military and defense technology can have irreparable consequences. For this reason, the basic components that make up the UAV must be under constant control. It should be monitored whether there is a malfunction in the motors, which are the most important parts of the UAV. Our main motivation is to propose an automatic real-time UAV motor fault detection method. Current and vibration signals have been used in the previous fault detection methods (see Section 1.3). More faults can be detected than current and voltage signals using sound signal, and also obtaining sound signals is easier and cheaper. Many deep learning-based methods have been proposed in the literature to detect UAV motor fault detection. However, large resources such as servers are needed for the implementation of deep learning methods. In the proposed method, statistical feature extraction and machine learning have been used together. Therefore, the computational complexity of our model is linear and it is a lightweight learning method. Moreover, our model can be implemented on the physical-world application easily and it can be implemented on an embedding system.

2.1. Literature review

UAV motors are widely used in both civil and military fields. Different faults may occur in UAV motors depending on operating conditions [2,3]. It is very important to detect and diagnose these faults earlier. There are many studies in the literature about UAV motor failures [4]. Looking at these studies, it is seen that only bearing, magnet, and eccentric failures could be detected [5,6].

* Corresponding author.
E-mail addresses: aaltinors@firat.edu.tr (A. Altinors), ferhatyol@gmail.com (F. Yol), orhanyaman@firat.edu.tr (O. Yaman).

https://doi.org/10.1016/j.apacoust.2021.108325
0003-682X/

Iannace et al. [7] proposed an Artificial Neural Network-based method for detecting faults in UAV propellers. The dataset was collected by using a sound level meter on the UAV. The quadrotor UAV was fixed on a tripod and operated. For balanced, unbalanced with one strip, and unbalanced with two strips, the microphone collected sound signals at four positions. By preprocessing the sound signals, 99.03% accuracy was calculated with an Artificial Neural Network. Magdaleno et al. [8] used sound signals to detect balance in UAV propellers. DWT decomposition was performed on the sound signals and the balance in the propeller was determined by spectral analysis. Balanced, one unbalanced, two unbalanced, three unbalanced and four unbalanced classes have been detected. Fu et al. [9] developed a hybrid method based on CNN-LSTM for six-rotor UAVs and performed fault detection. Accuracy was calculated for four datasets by applying DNN, CNN, LSTM, and CNN-LSTM methods. The highest result was obtained with the CNN-LSTM algorithm with 94.12%. Liu et al. [10] developed a sound-based diagnostic method for Quadrotors. The sound dataset was collected by creating different scenarios on Quadrotors. They created spectrograms from audio signals. Propeller failure was detected by using Spectrograms data with CNN. The magnitude of the propeller failure was also calculated. Zhang et al. [11] proposed a Time-Domain Frequency Estimation-based application for detecting UAV propeller failures. There are many studies in the literature for the detection of propeller failures in UAV motors [12,13]. In the literature, collecting sound signals with accuracy is very important while developing UAV audio-based diagnostic methods. Because of the acoustics of the sound change indoors and outdoors [14,15]. When collecting sound signals indoors, attention should be paid to the acoustics of the sound.

In the literature, besides sound-based condition monitoring and fault detection methods, vibration, current and voltage-based methods are also available. Bondyra et al. [16] performed condition monitoring and fault diagnosis for UAV propellers using signal processing. Signals were collected using an IMU sensor. Condition monitoring and fault detection were performed with the SVM classifier on the collected signals. According to Benini et al. [17] proposes an acceleration measurement-based method to detect VTOL-UAV propeller failures. Statistical methods were used for feature extraction. Tri-axial accelerations signals were collected with 1 kHz sampling. At the same time, location data with GPS is recorded on the SD card. Propeller failures were detected while performing Hovering, Climbing, Landing, and Complete flight movements on the VTOL-UAV. 95% accuracy was calculated while detecting faults. Cheng et al. [18] developed a vibration-based method for diagnosing quadcopter faults. In the model developed, they extracted features using RMS, Sample Entropy, and Standard Deviation algorithms from the three-axis vibration data obtained from the accelerometer. Later, in the Self Organization Map (SOM) model they developed using Tri-axial accelerometer data, they achieved 96.98% and 99.24% accuracy. Sadhu et al. [19] developed a neural network-based method for fault detection and identification. By using Bi-LTSM and CNN, flight data was classified and a fault diagnosis was made. In the experiments performed, fault detection was possible with 99.00% accuracy in simulation data and 85.00% accuracy in real-time experimental data. Lu et al. [20] proposed a deep learning-based method for fault detection in UAV motors. In the method they developed, the acceleration of the increase in motor temperatures was monitored and fault prediction was made. Bearing failures were determined from current and vibration data on an experimental setup. Current studies on detecting UAV motor faults are listed in Table 1.

As can be seen in Table 1, many sensors such as sound, IMU, temperature, current are used to detect malfunctions in UAV motors. Many methods such as machine learning, signal processing, and deep learning have been applied in the studies in the literature. Generally, propeller and balance faults are detected. In this study, propeller, eccentric and bearing failures can be detected. Since many types of faults can be detected simultaneously with sound-based methods, sound signals are used in this study. The main purpose of this study is to detect more than one type of fault. At the same time, it is to develop a lightweight method that can work on UAVs in real-time with high accuracy.

2.2. Our method

When the articles in the literature are scanned, it is seen that vibration, current, and voltage signals are mostly used for fault detection. But in fact, propeller and balance malfunctions are usually detected with these signals. But, in this study, by using sound signals, propeller, eccentric and bearing malfunctions in UAV motors are diagnosed. The use of vibration, current, and voltage signals together increases the complexity of the method, and it is also difficult to detect the mentioned faults. In the proposed method, many faults have been detected with high accuracy by using sound signals. Statistical equations have been used to extract properties from sound signals. DT, SVM, and KNN algorithms were used for the classification of the obtained features. The reason why statistical equations and machine learning methods are preferred in the proposed method is that the method can work quickly. Malfunctions that occur during the flight of UAVs should be diagnosed early. For this reason, a real-time method has been developed that is compatible with embedded systems that can be used on UAV.

2.3. Contributions and novelties

In this study, an acoustic-based method is proposed for detecting propeller, eccentric and bearing failure, which are the most important components of UAV motors. The main contributions of the proposed method are summarized as follows.

- In the study, high-speed UAV motors are used. Sound signals received from DC motors are used for fault detection. On the basis of sound signals, more faulties can be detected.
- Statistical equations are used for feature extraction from sound signals. In the study, 1200×44100 sound signals were received. By using statistical equations, 1200×6 features are extracted from 1200×44100 sound signals. Thus, a fast method that can work in real time has been developed. A high automatic fault classification model has been proposed in this work using a lightweight machine learning technique.

2.4. Study outline

In the second part of this study, information about UAV motors is given. The motors used in the study are explained, and their properties are given. In the proposed method, feature extraction from sound signals received from motors is explained. In addition, machine learning methods and parameters used are given. In the fourth chapter, the experimental setup and classification results are presented. In the fifth chapter, the results of the proposed method are analyzed. In the conclusion part, the results of the method are explained.

3. Material

Brushless motors make the winding energy exchange with some electronic circuits instead of brush-collector. There are permanent magnets on the outer wall of conventional DC motors, and the windings in the rotor are energized in different positions with the help of a brush, creating opposite forces to each other,

Table 1
Literature review.

Studies	Fault Types	Dataset	Method	Accuracy
Wang et al. [21], 2020	General flight failures	Control Parameters	Quantified LSTM	95.1%
			FDMAE	98.6%
Sadhu et al. [19], 2020	General flight failures	GPS, Communication and Sensors	CNN's and LSTMs	90%
Titouna et al. [22], 2020	General flight failures	Control Parameters	Artificial Neural Networks	–
Liu et al. [10], 2020	Propeller Failure	Sound Data	Spectrogram & CNN	90%
Ghalamchi et al. [23], 2020	Propeller Failure	Vibration data (IMU)	Discrete Fourier transformation (DFT)	–
Kante et al. [24], 2020	Motors Failure	ESC PWM Signals	–	–
Ray et al. [25], 2020	Motor Winding Failure	Current Data	Discrete Wavelet Transform (DWT)	–
Cheng et al. [18], 2019	Motors Vibration Failure	Mems Accelerometer & Gyro	Machine Learning	96.8%
Keipour et al. [26], 2019	General flight failures	Control Parameters	Gaussian distribution	86.36%
Rangel et al. [8], 2019	Propeller Balancing Failure	Sound Data	Discrete Wavelet Transform (DWT)	–
Benini et al [17], 2019	Propeller Balancing Failure	IMU Data	Discrete Fourier transformation (DFT)	95%
Iannace et al. [7], 2019	Propeller Failure	Sound Data	Artificial neural networks	96%
Wang et al. [27], 2019	Motors and Propeller Failure	Vibration data	FFT, Hilbert Huang Transform (HHT)	–
Lu et al. [20], 2018	Motors Temperature Failure	Temperature Data	Deep Reinforcement learning	–
Pourpanah et al. [28], 2018	Motors and Propeller Failure	Vibration and Current Data	CART	95.8%
			KNN	96.4%
			NB	96.5%
			SVM	96.7%
			QFAM-GA	97.8%
Aboutalebi et al. [29], 2018	Sensors Failure	IMU Data	Artificial neural networks	–
Bondara et al. [16], 2017	Propeller Failure	IMU Data	FFT, Wavelet Packet Decomposition(WPT)Support Vector Machine(SVM)	–
Saied et al. [13], 2017	Motors Failure	Speed Data	SVM	–

Table 2
Technical specifications of Wester A2212 model UAV motors.

Model	Wester A2212 1400 KV	Wester A2212 2200 KV	Wester A2212 2700 KV
Operating voltage	2S-3S Li-po (7.4–11.1 V)	2S-3S Li-po (7.4–11.1 V)	2S-3S Li-po (7.4–11.1 V)
Current Capacity	12A(60S)	18.5A(60S)	18.5A(60S)
No load Current	10 V @ 0.5A	10 V @ 0.5A	10 V @ 1.8A
Maximum Efficiency	80%	82%	92%
Motor Dimensions	27.5x30mm	27.8x27mm	27x26mm
Weight	47gr	48gr	60gr
Shaft Diameter	3.17 mm	3.17 mm	3.17 mm

converting electrical energy into mechanical energy. But in brushless motors, the rotor and stator are in the opposite position. Since 1980 s, it has been preferred for applications that do not require much power, especially with the development of magnets and semiconductors. UAV motors are usually wound in 2 or 3 phases, but there are also brushless motors with more phases as well. There are 4 and 8 poles UAV motors with at least two poles. In this study, Wester A2212 model 1400 KV, 2200 KV, and 2700 KV UAV motors were used. The technical characteristics of the motors shown in Fig. 1 are given in Table 2.

Since the brushless motors used in UAVs are the types of motors operating at high speeds, malfunctions may occur during long-term operations. In UAV motors, rotor-shaft, bearing, and stator failures usually occur [30,31].

Fig. 1. Motors used in the study (a) Wester A2212 1400 KV (b) Wester A2212 2200 KV (c) Wester A2212 2700 KV.

3.1. Rotor-shaft faults

UAV motors are motor types that contain permanent magnets and whose operation is relatively not very complicated. These permanent magnets, which are placed in the rotor at a certain angle, follow the rotating field on the stator and rotate the rotor. These permanent magnets on the rotor are usually attached to the rotor using strong adhesives. Especially if the motor is impacted or operated with an unbalanced propeller, vibrations on the motor may cause permanent magnets to be out of position. A very small slip on the magnet can cause the motor to work with vibration and noise and decrease the motor efficiency and cause the motor to overheat [32]. At the same time, a physical impact that the motor may receive from the outside (generally the blows that may occur during crushing) may cause the motor shaft to bend; however, the motor balance may deteriorate. In this case, the motor will run in a loud and vibrating manner again.

Bearing faults

UAV motors used in UAVs are generally designed to allow good cooling with open windings. Although this design method has a positive effect on the cooling of the motor windings, it has negative effects on the bearings of the motors, especially in dusty environments. Dust particles in the air can cause the bearings to lose their properties in a short time and to operate noisily. At the same time, faulties on the Rotor and Shaft, and also the use of improperly balanced propellers cause vibrations on the motor. However, motor bearings deteriorate in a short time and may cause noisy operation [32].

Stator faults

Stator faults are usually caused by the breakdown of the stator winding insulation. There are several main reasons for these malfunctions. The most common of these situations is that the motor gets hotter than normal due to the overload. In such overload situations, because excessive current will flow through the motor windings, there is more heating of the windings. If the high heat generated in the windings is not thrown out of the motor in a short time, the insulation on the windings will deteriorate and cause the motor to burn and become inoperable [32].

Propeller faults

In the event that unmanned aerial vehicles hit any obstacle during their flight, breakage or deterioration of the wings may occur. This prevents the UAV from flying correctly [33]. In this study, fault types are created by using three different UAV motors. These failures are Propeller, Eccentric and Bearing failures. The experimental setup developed in the study is shown in Fig. 2.

This process is repeated for three different speed UAV motors. Thus, four classes of sound data are obtained for three motors. A Samsung mobile phone and an external microphone connected it were used while collecting sound data from the running motors. Thus, it was aimed to collect better quality audio dataset. The following are the specifications of the external microphone used:

- Polarity: Omnidirectional
- Frequency range: 65 Hz–44KHz
- Signal/Noise: 74 dB SPL
- Output impedance: 1000 Ohms or less
- Connector: 3.5 mm stereo jack
- Battery type: LR44

The sound was collected with the "Voice Recorder" program on the phone. While creating sound data, AAC (m4a) format, 320 kbps, and 44 kHz sampling frequency were preferred [34]. A quiet laboratory of about 50 square meters was used to collect the sound signals from the motors. The microphone is fixed at a distance of about 1 m from the UAV motor. Being close to the UAV motor may adversely affect the audio dataset because it is indoor. For this reason, a large laboratory was used and a microphone was placed about 1 m away. A dataset was created in a noise-free environment for three different motor types. A total of 300 s of sound was collected for each failure condition. Since the recording frequency is 44 kHz, 300×44100 data were collected. This process was repeated for four classes, and 1200×44100 data were collected for each motor type. Sample sound signals obtained from the microphone in the study are shown in Fig. 3.

4. The proposed method

In this study, sound data were collected in four different conditions: Healthy motor, propeller failure, eccentric failure, and bearing failure. The block diagram of the proposed method is shown in Fig. 4.

4.1. Pre-Processing

There is a pre-processing step before extracting features from the sound data collected for three different motors. For preprocessing, the 1200×44100 sound data is normalized using Eq. (1).

$$Z' = \frac{Z - Z_{\min}}{Z_{\max} - Z_{\min}} \tag{1}$$

In Eq. (1), the Z value denotes the property. The values of Z_max and Z_min represent the maximum and minimum values in the array. After the normalization step, the sound data were arranged between 0 and 1. It has become suitable for feature extraction from sound data.

4.2. Feature extraction

Statistical equations are used for feature extraction from sound data. The Average, Standard Deviation, Variance, Correlation, Kurtosis, and Skewness values of 1200×44100 sound data were calculated. The statistical equations used in this study are given in Eqs. (2)–(7).

$$f1 = \frac{\sum_{i=1}^{N} X_i}{N} \tag{2}$$

$$f2 = \sqrt{\frac{\sum_{i=1}^{N} (X_i - f1)^2}{N}} \tag{3}$$

$$f3 = \frac{\sum_{i=1}^{N} (X_i - f1)^2}{N} \tag{4}$$

$$f4 = \sum_{i=1}^{N} \frac{i * X_i - f1}{\sigma_x} \tag{5}$$

$$f5 = \frac{\sqrt{N(N-1)}}{N-2} \left(\frac{\frac{1}{N}\sum_{x=1}^{N} (X_i - f1)^3}{\frac{1}{N}\sum_{x=1}^{N} (X_i - f1)^2} \right)^{3/2} \tag{6}$$

$$f6 = \frac{N-1}{(N-2)(N-3)} \left[(N+1) \left(\left(\frac{\frac{1}{N}\sum_{x=1}^{N} (X_i - f1)^4}{\frac{1}{N}\sum_{x=1}^{N} (X_i - f1)^2} \right) - 3 \right) + 6 \right] \tag{7}$$

In this study, statistical feature extraction was used for a real-time method [35]. Average, Standard Deviation, Variance, Correlation, Kurtosis, and Skewness values parameters were used for statistical feature extraction. Thus, 1200×6 features were calculated for the 1200×44100 dataset. As a result of feature extraction, 1200×6 features were obtained for three motor types.

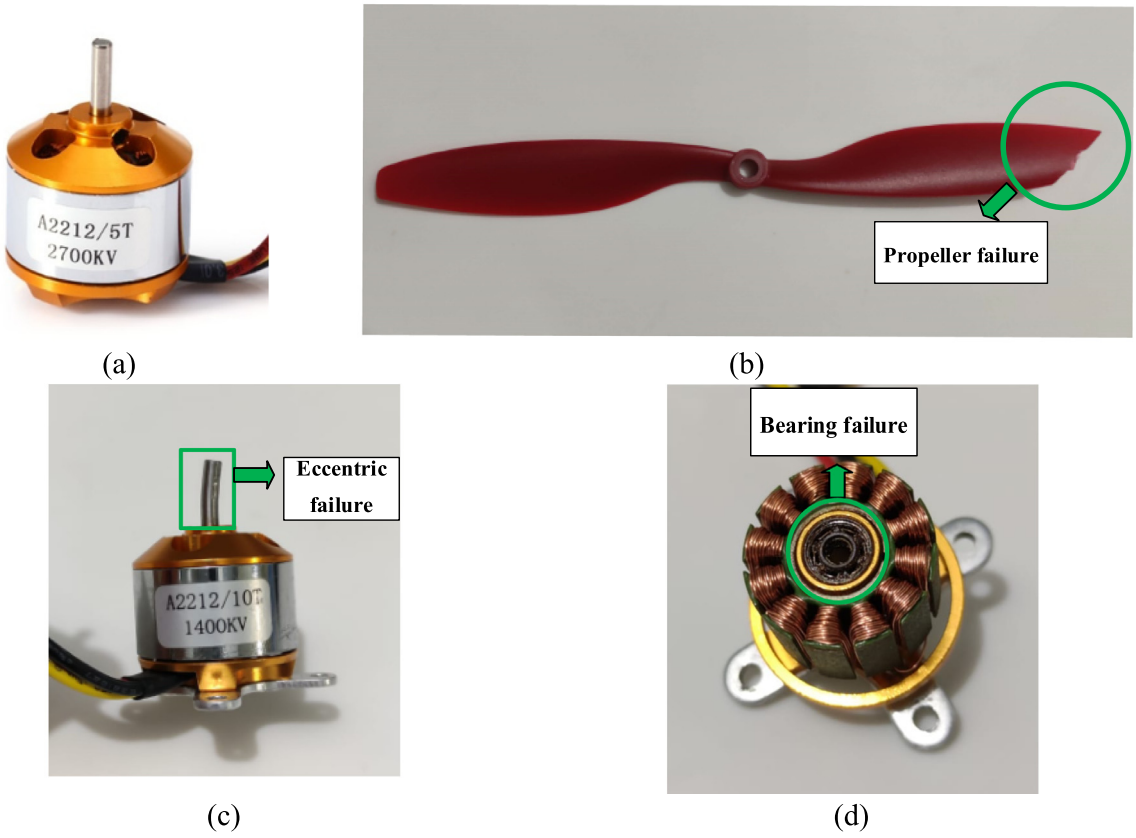

Fig. 2. Images of the experimental setup developed in this study (a) Healthy motor, (b) Propeller failure (c) Eccentric failure (d) Bearing failure.

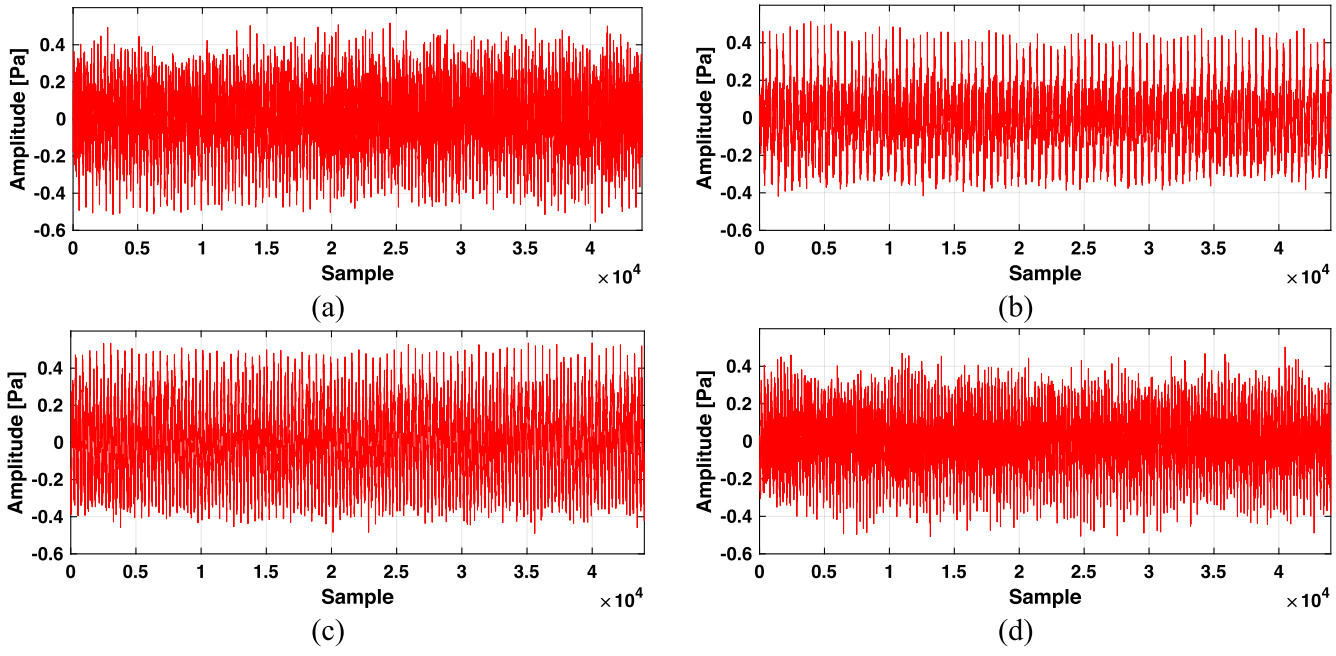

Fig. 3. Sound samples collected for fault detection (a) Healthy (b) Propeller failure (c) Eccentric failure (d) Bearing failure.

In the study, it was aimed to extract a small number of features. The reason for this is to develop a fast method that can work on embedded systems. The classification was made after feature extraction.

4.3. Classification methods

The properties obtained in the study were used together with the classification algorithms. The result of the classification algo-

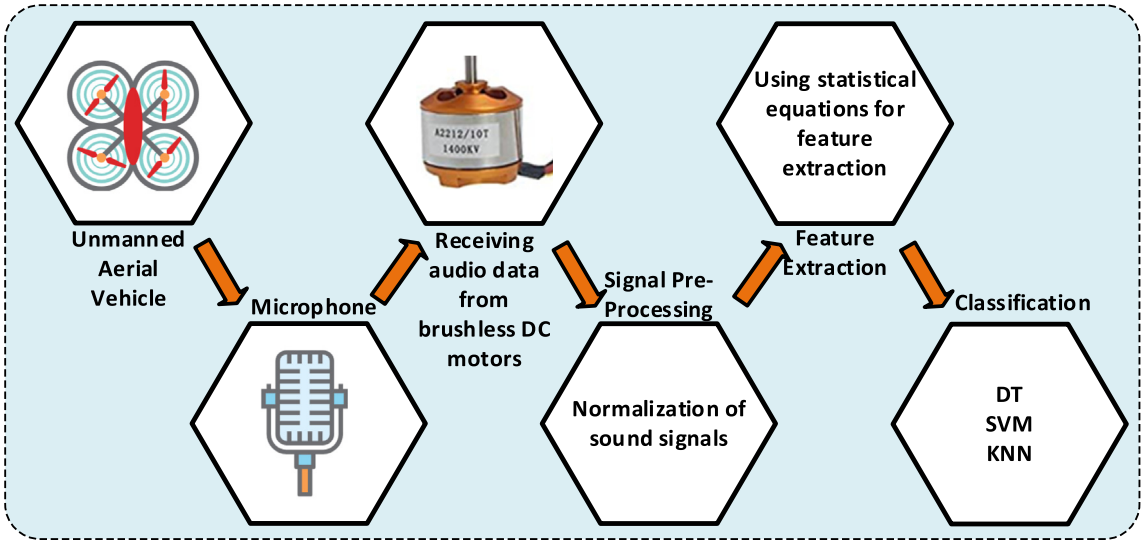

Fig. 4. Block diagram of the proposed method.

Table 3
Parameters of proposed classification methods.

Fine DT	Maximum number of splits	100
	Split criterion	Gini's diversity index
	Surrogate decision splits	Off
Quadratic SVM	Kernel function	Quadratic
	Box constraint level	2
	Kernel scale mode	Auto
	Manual kernel scale	1
	Multiclass method	One-vs-one
Medium KNN	Number of neighbors	10
	Distance metric	Euclidean
	Distance weight	Equal
	Standardize data	True

rithm gives the success of the method. DT, SVM, and KNN algorithms are used in the proposed method.

DT is a frequently used method in classification studies because the rules used in creating tree structures are simple and understandable. In the classification problem that needs to be solved with this method, it simply performs the decision-making process by dividing the data into sections. The data to be classified are classified and distributed sequentially into sub-sections until they reach a leaf, depending on the rule mechanism to be used while creating the decision tree. In order to understand the generalization ability of the created decision tree structure, test data are tested at the root of the tree and remain bound by a single decision rule until the data reach the bottom. It is possible to separate these groups by drawing a boundary between labeled groups in a plane for classification in the SVM algorithm. The place where the decision boundary to separate the planes will be drawn should be the farest place from the group members. Support Vector Machines set these limits. KNN algorithm is a method that is frequently used in machine learning applications and other classification applications due to its simple and strong structure. This method realizes the classification based on the proximity to the training examples in the feature space. The KNN algorithm performs class assignments according to the k value. Although the implementation of the method is simple and powerful, it is one of the disadvantages of this method that it requires a large memory space, and the processing load increases as a result of the increase in the volume of

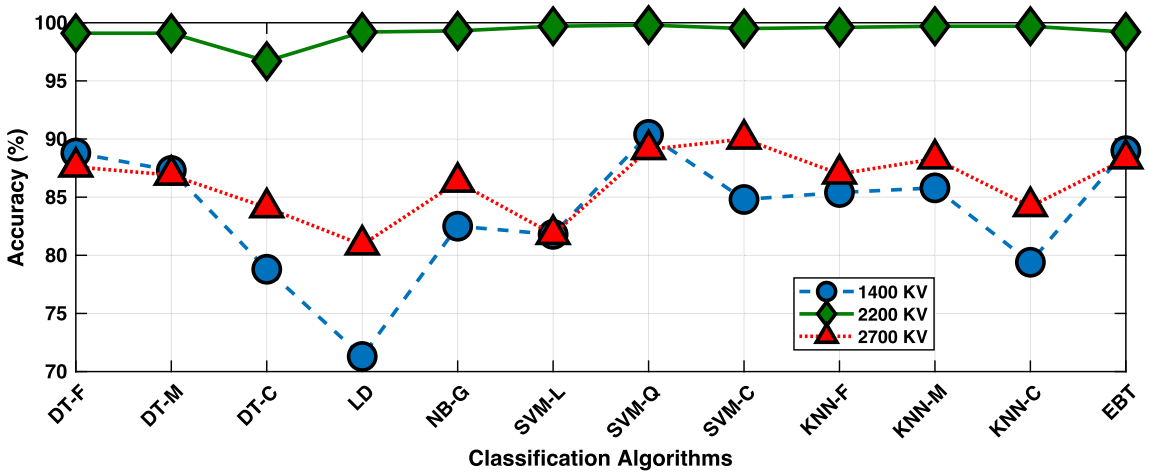

Fig. 5. The accuracy results calculated for Fine DT, Medium DT, Coarse DT, Linear Discriminant, Gaussian Naïve Bayes, Linear SVM, Quadratic SVM, Cubic SVM, Fine KNN, Medium KNN, Cosine KNN, and Ensemble Boosted Trees.

data. In the study, Fine_DT was preferred as the DT algorithm, Quadratic_SVM as the SVM algorithm, and Medium_KNN as the KNN algorithm. Classification parameters of Fine_DT, Quadratic_SVM and Medium_KNN algorithms are given in Table 3.

Fine DT, Medium KNN, and Quadratic SVM algorithms were used to classify the calculated features in the proposed method. The reason why these algorithms are preferred is that they are higher than the results of other algorithms. 12 classifiers have been used for classification. These classifiers are Fine DT, Medium DT, Coarse DT, Linear Discriminant, Gaussian Naïve Bayes, Linear SVM, Quadratic SVM, Cubic SVM, Fine KNN, Medium KNN, Cosine KNN, and Ensemble Boosted Trees. The accuracy results calculated for 12 classifiers are shown in Fig. 5.

As can be seen in Fig. 5, Fine DT, Medium KNN and Quadratic SVM were preferred among these classifications with high accuracy.

5. Experimental results

The proposed method in the study was developed in the MATLAB 2020a program. Results were obtained from a computer with i7-9700 CPU 3.00 GHz processor, 32 GB RAM and 6 GB Video card. A four motor quadrotor was used in the experimental setup. Propeller, eccentric, and bearing failures were created for this quadrotor, and sound data was created. Dataset has sound data of four classes: Healthy, propeller, eccentric, and bearing. This process has been applied for Wester A2212 model 1400 KV, 2200 KV and 2700 KV UAV motors. Thus, four classes of sound data are generated for three types of UAV motors.

The proposed method was applied to the sound data, and the ROC curves given in Fig. 6 were calculated.

The best ROC curve for 1400 KV motor, as can be seen in Fig. 6, is AUC = 0.97. This ROC curve is calculated by the SVM algorithm.

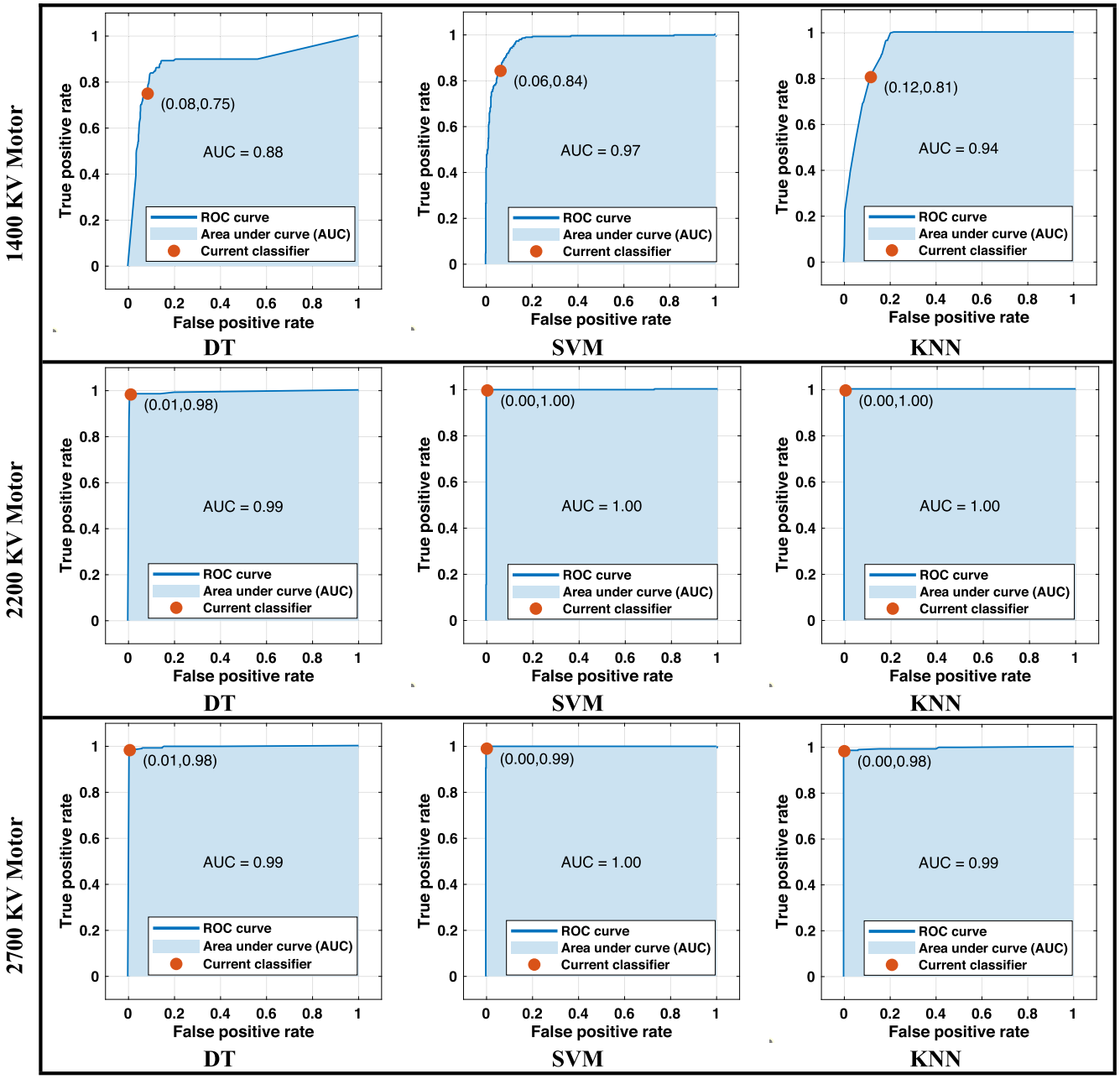

Fig. 6. ROC curves obtained in classification of faults in 1400 KV, 2200 KV and 2700 KV UAV motors.

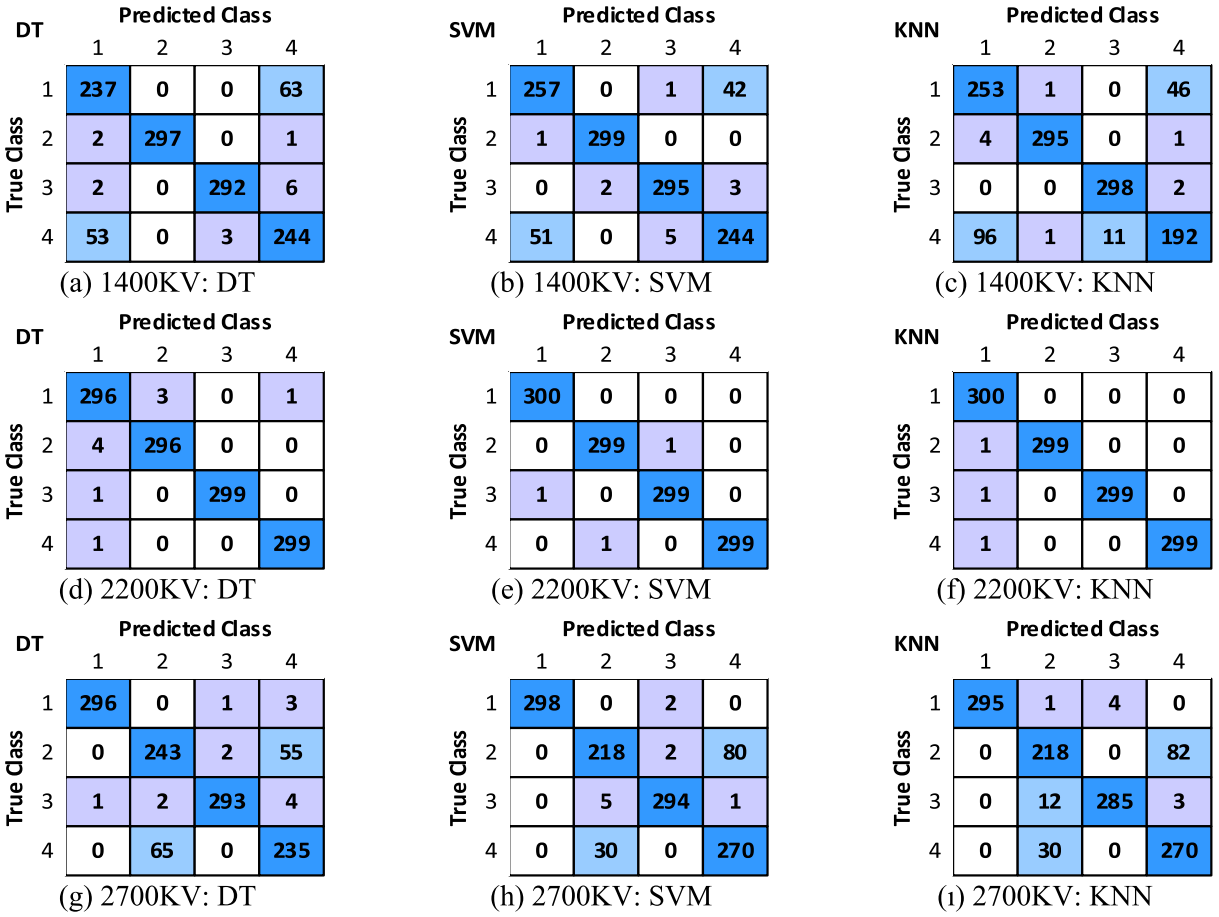

Fig. 7. Confusion matrix calculated for classification of faults in 1400 KV, 2200 KV and 2700 KV UAV motors.

The best ROC curve for 2200 KV motors obtained from SVM and KNN algorithms is AUC = 1.00. The best ROC curve for 2700 KV motor is AUC = 1.00. This ROC curve is calculated with the SVM algorithm as in a 1400 KV motor. It is calculated as AUC = 0.99 for 2700 KV motor by DT and KNN algorithms. The proposed method was run with 1000 iterations, and the confusion matrix obtained was shown in Fig. 7.

As can be seen in Fig. 7, the best classification for 1400 KV motor is calculated with the SVM algorithm. When viewed on a class basis, the highest value for Healthy (Class 1) and Propeller (Class 2) classes was obtained with the SVM algorithm. The highest value for the eccentric (Class 3) class was obtained with KNN. The highest value for the bearing (Class 4) class was calculated with DT and SVM. The highest results for the 2200 KV motor were calculated with SVM and KNN algorithm. For 2700 KV motor, SVM for Healthy (Class 1), DT for Propeller (Class 2), SVM for Eccentric (Class 3), SVM and KNN for Bearing (Class 4), the highest classification was calculated. For 1400 KV, 2200 KV, and 2700 KV UAV motors, DT, SVM, and KNN algorithms were run 1000 iterations and Accuracy (*CACC*), Unweighted Average Precision (*UAP*), Unweighted Average Recall (*UAR*), Geometric mean (*GM*), F-measure (*F1*) and *IoU* parameters were calculated. These parameters are given in Eqs. (8)–(13), respectively.

$$CACC = \frac{TP_c + TN_c}{TP_c + TN_c + FP_c + FN_c}, c = \{1, 2, \cdots NC\} \tag{8}$$

$$UAP = \frac{1}{NC}\sum_{c=1}^{NC}\frac{TP_C}{TP_c + FP_c} \tag{9}$$

$$UAR = \frac{1}{NC}\sum_{c=1}^{NC}\frac{TP_C}{TP_c + FN_c} \tag{10}$$

$$GM = \sqrt[NC]{\prod_{c=1}^{NC}\frac{TP_c}{TP_c + FN_c}} \tag{11}$$

$$F1 = \frac{2 * (UAP * UAR)}{UAP + UAR} \tag{12}$$

$$IoU = \frac{TP_c}{TP_c + FP_c + FN_c}, c = \{1, 2, \cdots NC\} \tag{13}$$

Where TPC, TNT, FPC, and FN_c are the number of true positives, true negatives, false positives, and false negatives, respectively. N_c is the number of classes. The results obtained for 1400 KV, 2200 KV, and 2700 KV Brushless DC motors are given in Table 4.

As seen in Table 4, the highest accuracy value for a 1400 KV motor was calculated as 91.25% with the SVM algorithm. In DT and KNN algorithms, accuracy values were calculated as 89.16% and 86.50%, respectively. For the 2200 KV motor, the highest accuracy value was calculated as 99.75% by SVM and KNN algorithms. With the DT algorithm, the highest accuracy value is 99.16%. For the 2700 KV motor, the highest accuracy value was calculated as 90.00% with the SVM algorithm. In DT and KNN algorithms, accuracy values were calculated as 88.91% and 89.00%, respectively. Accuracy, precision, recall, geometric mean, F1-measure, and IoU results obtained from the proposed method were examined, and it was seen that the highest results were calculated for 2200 KV.

Table 4
Accuracy, precision, recall, geometric mean, F1-measure, and IoU (%) results of the used 3 classifiers.

Case	Classification	Parameter	Accuracy	Precision	Recall	Geo-mean	F1-measure	IoU
1400 KV	DT	Max	89.16	89.32	89.16	88.70	89.24	100
		Min	85.08	85.23	85.08	84.04	85.15	97.79
		Mean	86.89	86.98	86.89	56.16	86.93	99.05
		Std	0.59	0.60	0.59	0.67	0.59	0.33
	SVM	Max	91.25	91.27	91.25	90.90	91.26	99.61
		Min	89.50	89.46	89.50	89.00	89.48	98.06
		Mean	90.45	90.44	90.45	90.04	90.45	99.32
		Std	0.29	0.29	0.29	0.31	0.29	0.28
	KNN	Max	86.50	86.78	86.50	85.21	86.63	99.59
		Min	83.50	83.58	83.50	81.60	83.54	96.38
		Mean	85.11	85.30	85.11	83.62	85.20	98.05
		Std	0.45	0.47	0.45	0.54	0.46	0.49
2200 KV	DT	Max	99.16	99.16	99.16	99.16	99.16	98.01
		Min	98.25	98.25	98.25	98.23	98.25	94.17
		Mean	98.78	98.79	98.78	98.78	98.78	96.22
		Std	0.15	0.15	0.15	0.15	0.15	0.60
	SVM	Max	99.75	99.75	99.75	99.74	99.75	100
		Min	99.33	99.33	99.33	99.33	99.33	98.34
		Mean	99.60	99.61	99.60	99.60	99.60	99.25
		Std	0.06	0.06	0.06	0.06	0.06	0.33
	KNN	Max	99.75	99.75	99.75	99.74	99.75	99.66
		Min	99.58	99.58	99.58	99.58	99.58	99.00
		Mean	99.66	99.66	99.66	99.66	99.66	99.33
		Std	0.01	0.01	0.01	0.01	0.01	0.02
2700 KV	DT	Max	88.91	89.04	88.91	88.42	88.97	100
		Min	84.33	84.49	84.33	83.27	84.41	98.64
		Mean	86.86	87.01	86.86	86.19	86.93	99.51
		Std	0.64	0.64	0.64	0.72	0.64	0.29
	SVM	Max	90.0	90.43	90.0	89.32	90.21	100
		Min	87.66	88.18	87.66	86.66	87.92	99.32
		Mean	88.93	89.44	88.93	88.11	89.19	99.92
		Std	0.29	0.30	0.29	0.33	0.29	0.15
	KNN	Max	89.00	89.55	89.00	88.40	89.27	100
		Min	87.25	87.76	87.25	86.48	87.50	99.66
		Mean	88.19	88.74	88.19	87.53	88.47	99.66
		Std	0.28	0.29	0.28	0.31	0.28	0.02

Table 5
Time of feature extraction, training, and test operations for DT, SVM, and KNN algorithms.

	DT		SVM		KNN	
	Mean (ms)	Std (ms)	Mean (ms)	Std (ms)	Mean (ms)	Std (ms)
Feature Extraction	4.14	0.03	4.14	0.03	4.14	0.03
Training (10-Fold CV)	169.5	68.2	1353.8	147.7	181.1	67.3
Test Model	26.0	24.4	36.0	28.7	28.5	25.4
Total Training	173.6	–	1357.94	–	185.24	–
Total Test	30.14	–	40.14	–	32.64	–

Running times of feature extraction, training, and test processes for DT, SVM, and KNN algorithms are calculated in Table 5.

As seen in Table 5, the feature extraction step is equal in all algorithms. After the feature extraction process, training was carried out with 10-Fold CV. It is the DT algorithm that completes the fastest training process. Then it performs the KNN algorithm training step with 181.1 ms. SVM algorithm is very slow compared to DT and KNN algorithm. The fastest algorithm for the test step is DT algorithm with 26 ms. The test step was calculated as 36 ms with the SVM algorithm and 28.5 ms with the KNN algorithm. The total test time of 1×44100 sound data received in 1 s was 30.14 ms with DT algorithm, 40.14 ms with SVM algorithm, and 32.64 ms with KNN algorithm. When the total training and total test times of the proposed method are examined, it is clearly seen that DT is the fastest algorithm. It is seen that the KNN algorithm is also fast. The slowest algorithm is calculated as SVM. When the performances of the algorithms are examined in Tables 4 and 5, it is seen that DT and KNN algorithms are better. Although high success is achieved with the SVM algorithm, it is slower than other algorithms. As a result, DT and KNN algorithms are more suitable for real-time operation in embedded systems.

In the proposed method, 10 Fold Cross-validation was used and the results were calculated. In Fig. 8, the results for DT and BT algorithms were calculated by fold-wise accuracies.

6. Discussion

Class by class results are calculated for three different motor types used in the study. The obtained graphics are shown in Fig. 9.

The highest class by the class result for the 1400 KV UAV motor has been obtained for Propeller (Class 2) and Eccentric (Class 3) classes. For Class 2, the highest accuracy value, with 99.66% was calculated by the SVM algorithm. For Class 3, the highest accuracy value with 99.33% was obtained by the KNN algorithm. All classes gave high results for the 2200 KV UAV motor. The lowest accuracy value for Class 2 was calculated with 97.33% by DT algorithm. All accuracy values for other classes are higher than 98%. The class's highest class result for the 2700 KV UAV motor is calculated for

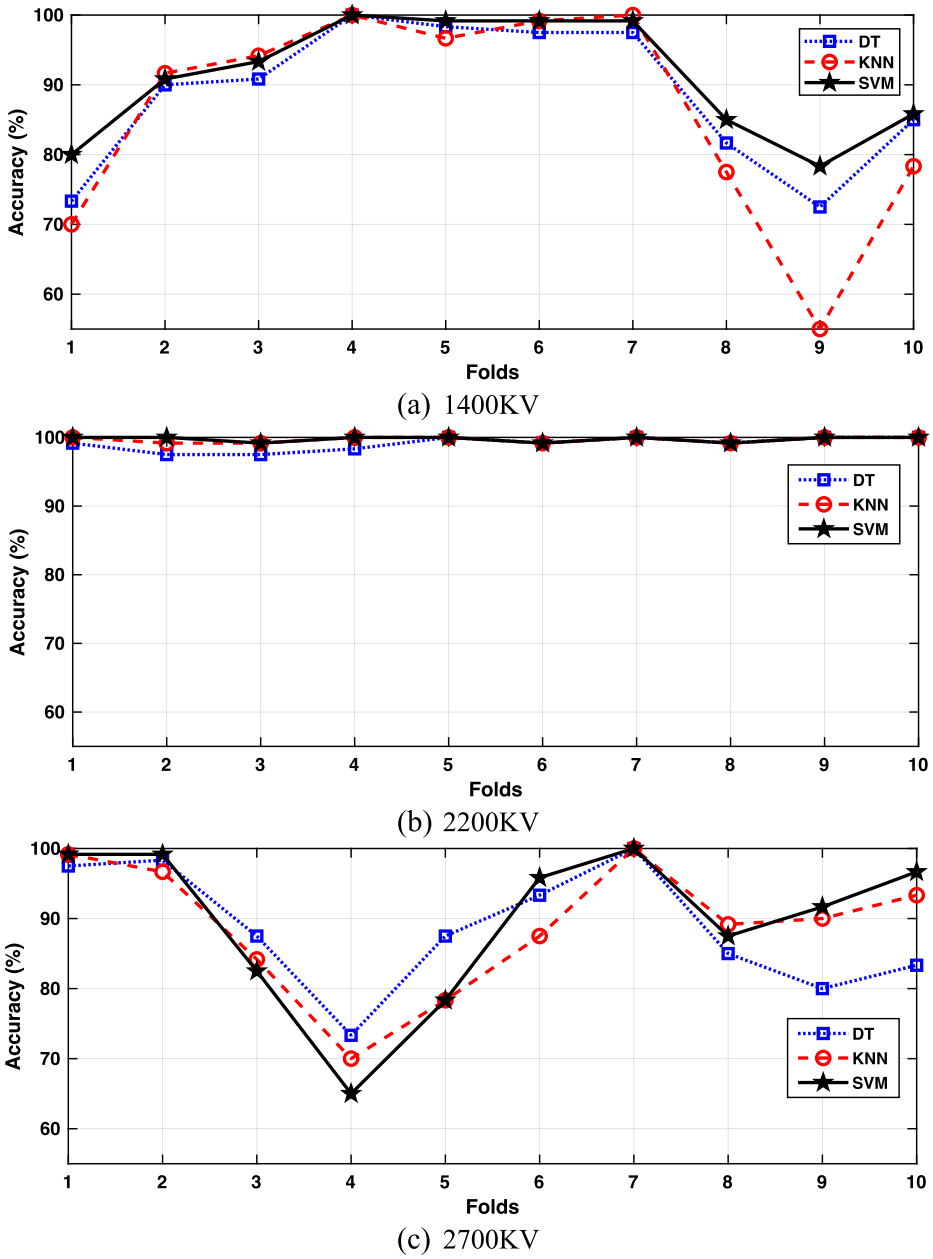

Fig. 8. The calculated fold-wise accuracies employing DT, KNN and SVM classifiers of the defined 1400 KV, 2200 KV and 2700 KV.

Healthy (Class 1) and Eccentric (Class 3). When the class by class results obtained for three motor types were examined, it was seen that the best results were obtained with a 2200 KV motor. Class2 and Class3 for 1400 KV and Class1 and Class3 for 2700 KV motor have the highest values. The accuracy values of Class 4 for the 1400 KV motor and Class 2 for the 2700 KV motor are low. It is thought that the reason for this situation may be that it was affected by the noise in the environment while creating the dataset or that the artificially created faults were not sufficiently formed. The Scatter Plot graphs are given in Fig. 10 verify the class by class results.

Three types of motors are used in the proposed method. Sound data was created by operating the 1400 VK DC motor at approximately 40% speed. The 2200 KV motor was operated at about 60%, and the 2700 VK motor at about 80% speed. As can be seen in Table 6, the faults in the 2200 KV motor are classified with 99.16%, 99.75%, and 99.75% accuracy, respectively, by DT, SVM, and KNN algorithms. In other motors, the accuracy is slightly lower. The difference in this accuracy value is related to the running speed of the motors. In future studies, the motors will be operated at different speeds, and methods will be developed for troubleshooting. When compared with the studies in the literature, it is seen that the proposed method is efficient. The proposed method is highly accurate and fast. This shows that the proposed method can be applied to the embedded system. The lightweight of the method provides fast classification. Thus, it will be able to work on embedded systems in real-time.

7. Conclusions

In this study, the classification of faults in UAV motors commonly used in UAVs is discussed. The importance of UAVs in both military and civilian fields has been the motivation of our work. In order to diagnose the malfunctions in the motors used in UAVs,

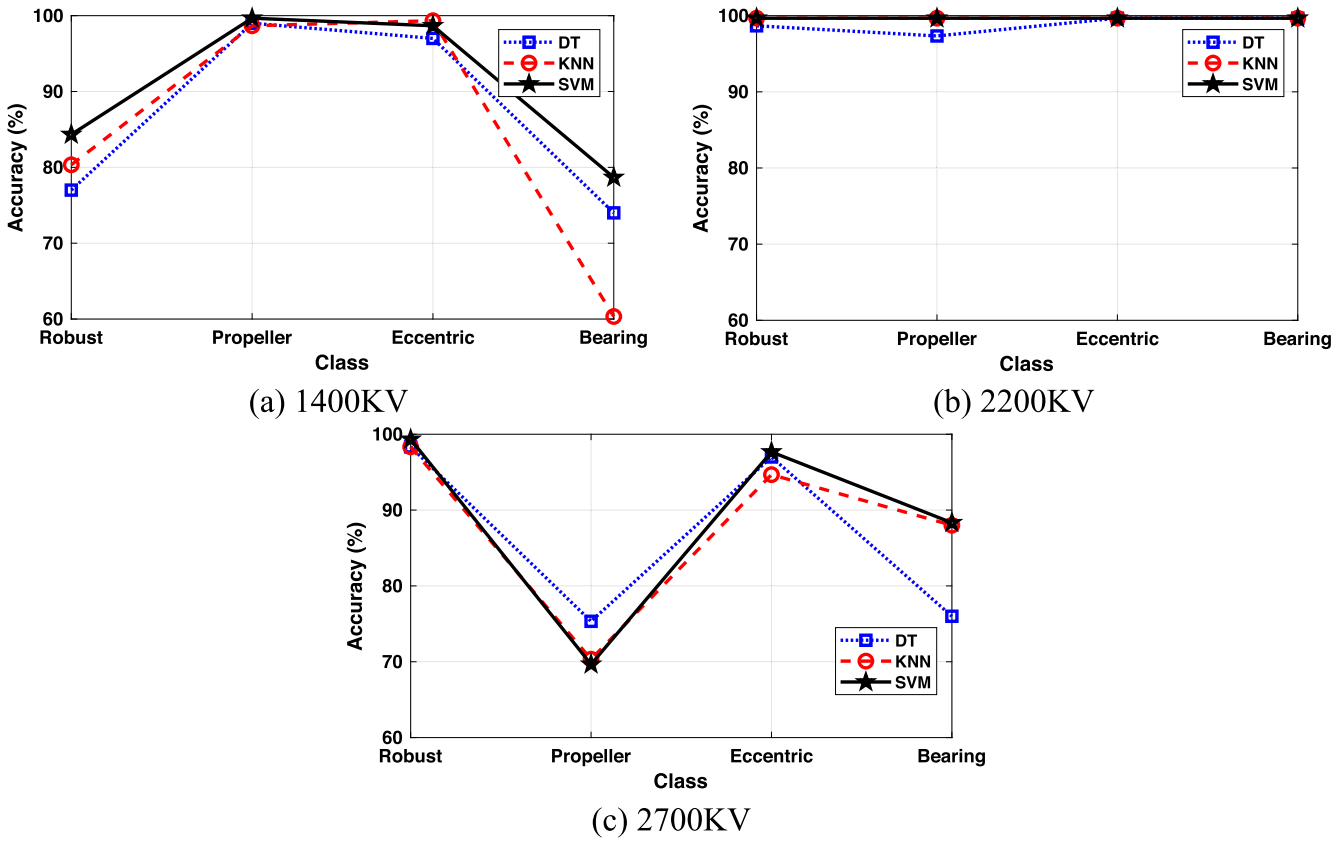

Fig. 9. Classification accuracies (%) obtained for various classes using our proposed method with BLDC acoustic datasets.

Table 6
Comparison of the proposed method with similar studies in the literature.

Studies	Fault Types	Features	Program	Method	Accuracy	Time (ms)
Sadhu et al. [19], 2020	General flight failures	i7-3.4 GHz, 8 GB RAM	AirSim drone simulator	CNN's and LSTMs	90%	82
		1.2 GHz, 1 GB RAM	Raspberry Pi 3 Model B and			312
		2 GHz, 8 GB RAM	Nvidia Jetson TX2			83
Liu et al. [10], 2020	Propeller Failure	–	MATLAB	Spectrogram & CNN	90%	–
Park et al. [36], 2020	Motors Failure	i7- 9700 K- 3.60 GHz	MATLAB	Linear discriminant analysis	30.35%	–
				Principal component analysis	86.43%	–
				Multi-principal component analysis	90.35%	–
				Fisher discriminant analysis	83.08%	–
				Partial least squares regression	98.04%	–
				Canonical variate analysis	96.92%	–
Cheng et al. [18], 2019	Motors Vibration Failure	–	–	Machine Learning	96.8%	–
Keipour et al. [26], 2019	General flight failures	2 GHz, 8 GB RAM	Nvidia Jetson TX2	Gaussian distribution	86.36%	2020
Wang et al. [21], 2020	General flight failures	–	Jetson Nano ARM Airbone ECP	LSTM	95.1%	2612
				PCA-LSTM	98.6%	2588
Our Method	Study	i7-3.00 GHz, 32 GB	MATLAB	DT	89.16%	30.14
1400 KV	Propeller failure	RAM		SVM	91.25%	40.14
	Eccentric failure			KNN	86.5%	32.64
Our Method	Bearing failure			DT	99.16%	30.14
2200 KV				SVM	99.75%	40.14
				KNN	99.75%	32.64
Our Method 2700 KV				DT	88.91%	30.14
				SVM	90.0%	40.14
				KNN	89.0%	32.64

artificial faults have been created over the sample motors. The sound dataset was created by creating malfunctions according to different motor types. Feature extraction has been made from these data, and a fast algorithm has been developed. The results are obtained by using the obtained properties together with DT, SVM, and KNN algorithms. MATLAB2020a software was used to

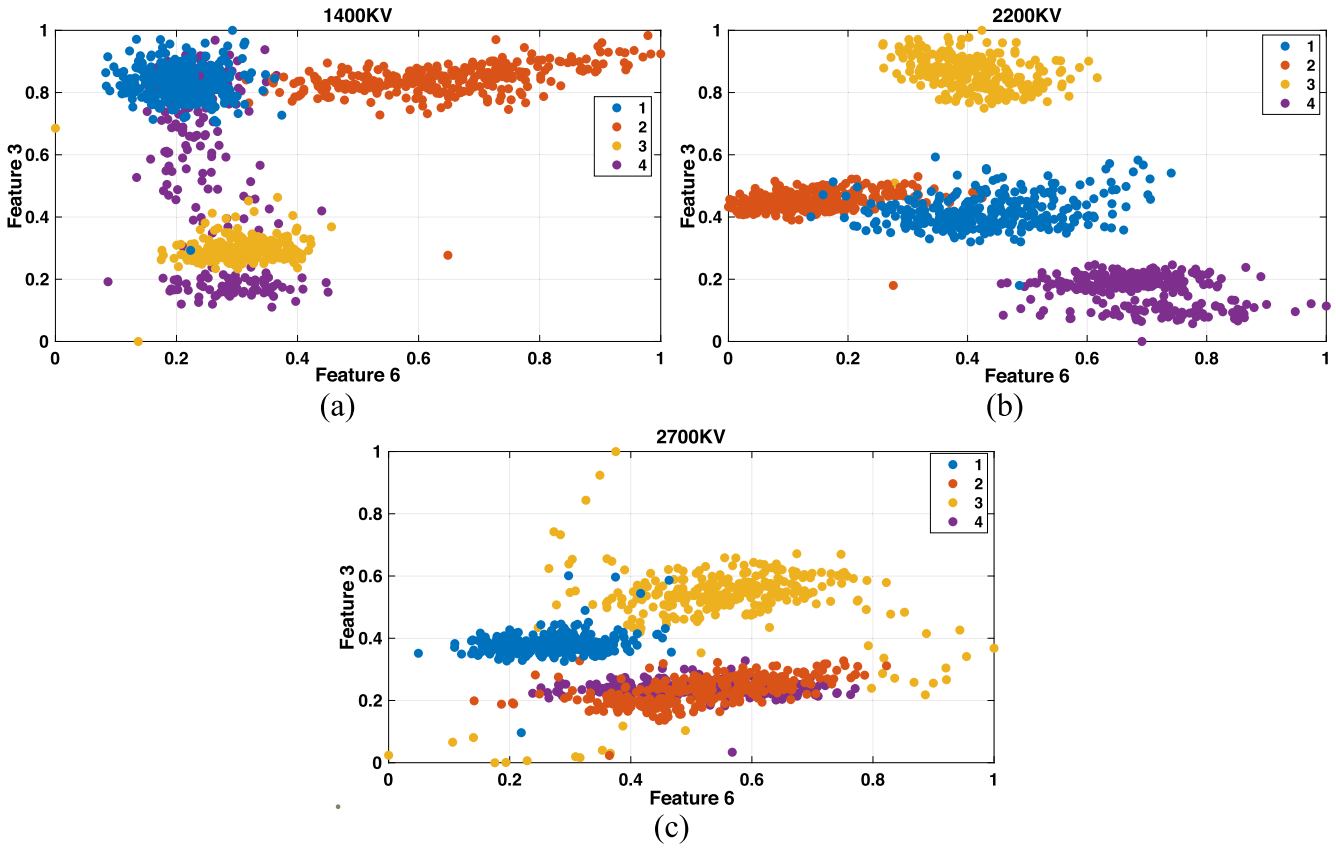

Fig. 10. Scatter plots of the selected features (a) 1400 KV (b) 2200 KV (c) 2700 KV. The comparison of the proposed method with similar studies in the literature is shown in Table 6.

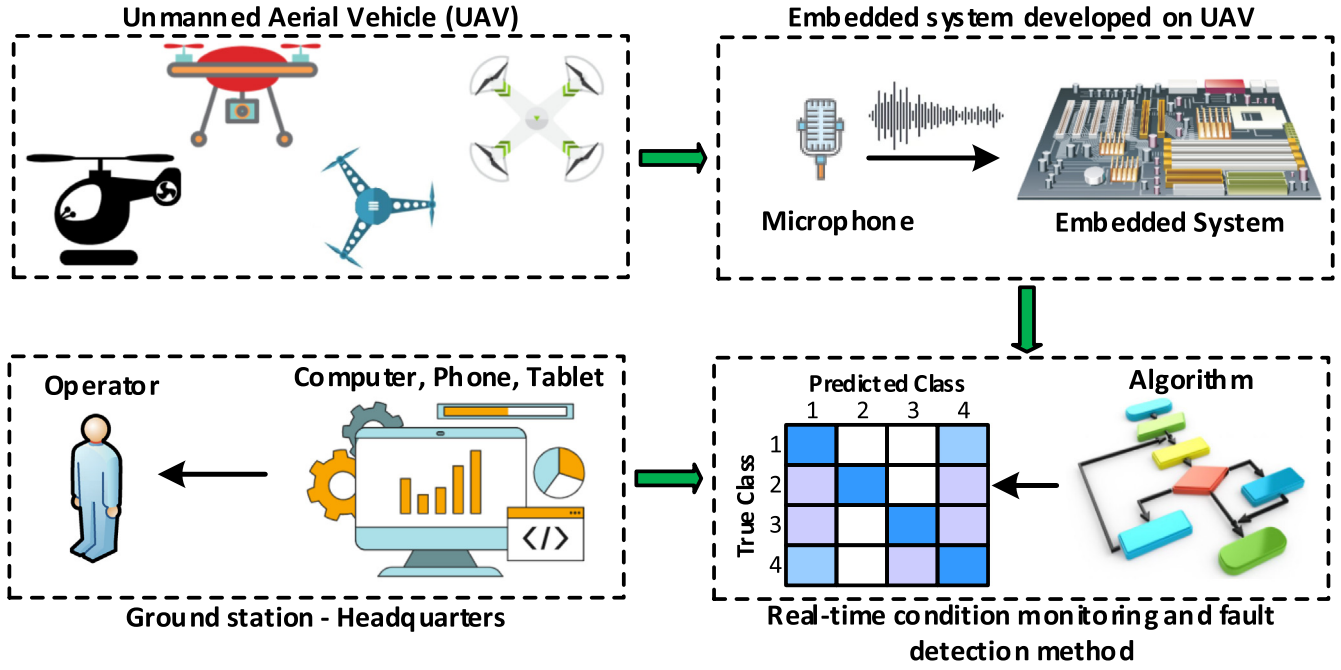

Fig. 11. Real-time fault detection method for UAV motors considered for future studies.

test the proposed method. For 1400 KV motor, 89.16%, 91.25%, and 86.5% accuracy was calculated from DT, SVM, and KNN algorithms. For the 2200 KV motor, the accuracy of 99.16%, 99.75%, and 99.75% was calculated from DT, SVM, and KNN algorithms, respectively. For the 2700 VK motor, 88.91%, 90.0%, and 89.0% accuracy were obtained, respectively. In addition, the classification test times of these algorithms are calculated as 30.14 ms, 40.14 ms, and 32.64 ms, respectively.

As a result of this study, a real-time method has been developed with the proposed statistical-based feature extraction and machine learning methods. The proposed method has been tested in a laboratory environment. Datasets were collected for three different speed motor types using an external microphone connected to the phone. When the accuracy and the working time of the algorithm are examined, it is seen that it can work in real-time.

8. Future works

Unmanned Aerial Vehicles are used in both military and civilian fields, especially in defense technology. The use of UAVs for imaging and defense purposes further increases the interest in these vehicles. High-speed brushless motors are used in UAVs. Failures in these motors cause big problems. In the next study, the proposed method will be applied to the embedded system and transformed into a real-time diagnostic application. In this study, the dataset was created by operating the motors sequentially while receiving the sound data. In the next study, while the sound is received from the faulty motor, other motors will also run in the background. This will eliminate background sounds from other motors while working in real-time. Different methods will be developed in order not to be affected by environmental conditions. The real-time fault detection method we are considering as our further studies for UAV motors is shown in Fig. 11.

As can be seen in Fig. 11, it will be tested on UAVs with different rotor numbers in future studies. The lightweight, high-accuracy and fast method developed in this study can be loaded into the embedded card. Thus, the real-time condition of the UAV can be monitored with the microphone and embedded card fixed on the UAV. In case of any abnormality/fault, our intended UAV condition monitoring system can send alerts to users.

Declaration of Competing Interest

The authors declare that they have no known competing financial interests or personal relationships that could have appeared to influence the work reported in this paper.

Acknowledgments

This work is supported by Firat University Research Fund, Turkey. Project Numbers: TBMYO.20.01.

References

[1] Olson IJ, Atkins EM. Qualitative failure analysis for a small quadrotor unmanned aircraft system. AIAA Guid Navig Control Conf 2013:1–11. https://doi.org/10.2514/6.2013-4761.
[2] Mitronikas E, Papathanasopoulos D, Athanasiou G, Tsotoulidis S. Hall-effect sensor fault identification in brushless DC motor drives using wavelets. Proc 2017 IEEE 11th Int Symp Diagnostics Electr Mach Power Electron Drives, SDEMPED 2017 2017;2017-Janua:434–40. 10.1109/DEMPED.2017.8062391.
[3] Ciaburro G, Iannace G. Improving smart cities safety using sound events detection based on deep neural network algorithms. Informatics 2020;7(3):23. https://doi.org/10.3390/informatics7030023.
[4] Faiz J, Jafari A. Interturn fault diagnosis in brushless direct current motors - A review. Proc IEEE Int Conf Ind Technol 2018;2018-Febru:437–44. 10.1109/ICIT.2018.8352217.
[5] Medeiros RLV, Filho ACL, Ramos JGGS, Nascimento TP, Brito AV. A novel approach for speed and failure detection in brushless DC motors based on chaos. IEEE Trans Ind Electron 2019;66(11):8751–9. https://doi.org/10.1109/TIE.4110.1109/TIE.2018.2886766.
[6] Veras FC, Lima TLV, Souza JS, Ramos JGGS, Lima Filho AC, Brito AV. Eccentricity failure detection of brushless DC motors from sound signals based on density of maxima. IEEE Access 2019;7:150318–26. https://doi.org/10.1109/Access.628763910.1109/ACCESS.2019.2946502.
[7] Iannace G, Ciaburro G, Trematerra A. Fault diagnosis for UAV blades using artificial neural network. Robotics 2019;8(3):59. https://doi.org/10.3390/robotics8030059.
[8] Rangel-Magdaleno JDJ, Urena-Urena J, Hernandez A, Perez-Rubio C. Detection of unbalanced blade on UAV by means of audio signal. 2018 IEEE Int Autumn Meet Power, Electron Comput ROPEC 2018 2019:2–6. 10.1109/ROPEC.2018.8661459.
[9] Fu J, Sun C, Yu Z, Liu L. A hybrid CNN-LSTM model based actuator fault diagnosis for six-rotor UAVs. Proc 31st Chinese Control Decis Conf CCDC 2019 2019:410–4. 10.1109/CCDC.2019.8832706.
[10] Liu W, Chen Z, Zheng M. An Audio-Based Fault Diagnosis Method for Quadrotors Using Convolutional Neural Network and Transfer Learning. Proc Am Control Conf 2020;2020-July:1367–72. 10.23919/ACC45564.2020.9148044.
[11] Zhang X, Luo H, Li K, Kaynak O. Time-domain frequency estimation with application to fault diagnosis of the UAVs blade damage. IEEE Trans Ind Electron 2021;0046:1. https://doi.org/10.1109/tie.2021.3084177.
[12] Lee Jun-yong, Lee Won-tak, Ko Sang-ho, Oh Hwa-suk. Fault classification and diagnosis of UAV motor based on estimated nonlinear parameter of steady-state model. Int J Mech Eng Robot Res 2020:22–31. https://doi.org/10.18178/ijmerr10.18178/ijmerr.10.1.22-31.
[13] Saied Majd, Lussier Benjamin, Fantoni Isabelle, Shraim Hassan, Francis Clovis. Fault diagnosis and fault-tolerant control of an octorotor UAV using motors speeds measurements. IFAC-PapersOnLine 2017;50(1):5263–8. https://doi.org/10.1016/j.ifacol.2017.08.468.
[14] Iannace Gino, Ciaburro Giuseppe, Trematerra Amelia. Acoustical unmanned aerial vehicle detection in indoor scenarios using logistic regression model. Build Acoust 2021;28(1):77–96. https://doi.org/10.1177/1351010X20917856.
[15] Ciaburro Giuseppe, Iannace Gino, Trematerra Amelia. Research for the presence of unmanned aerial vehicle inside closed environments with acoustic measurements. Buildings 2020;10(5):96. https://doi.org/10.3390/buildings10050096.
[16] Bondyra A, Gasior P, Gardecki S, Kasinski A. Fault diagnosis and condition monitoring of UAV rotor using signal processing. Signal Process - Algorithms, Archit Arrange Appl Conf Proceedings, SPA 2017;2017-Septe:233–8. 10.23919/SPA.2017.8166870.
[17] Benini A, Ferracuti F, Monteriu A, Radensleben S. Fault detection of a vtol uav using acceleration measurements. 2019 18th Eur Control Conf ECC 2019 2019:3990–5. 10.23919/ECC.2019.8796198.
[18] Cheng DL, Lai WH. Application of self-organizing map on flight data analysis for quadcopter health diagnosis system. Int Arch Photogramm Remote Sens Spat Inf Sci – ISPRS Arch 2019;42:241–6. https://doi.org/10.5194/isprs-archives-XLII-2-W13-241-2019.
[19] Sadhu V, Zonouz S, Pompili D. On-board deep-learning-based unmanned aerial vehicle fault cause detection and identification. Proc – IEEE Int Conf Robot Autom 2020:5255–61. https://doi.org/10.1109/ICRA40945.2020.9197071.
[20] Lu Huimin, Li Yujie, Mu Shenglin, Wang Dong, Kim Hyoungseop, Serikawa Seiichi. Motor anomaly detection for unmanned aerial vehicles using reinforcement learning. IEEE Int Things J 2018;5(4):2315–22.
[21] Wang B, Peng X, Jiang M, Liu D. Real-time fault detection for UAV based on model acceleration motor. IEEE Trans Instrum Meas 2020;69:9505–16. https://doi.org/10.1109/TIM.2020.3001659.
[22] Titouna C, Nait-Abdesselam F, Moungla H. An Online Anomaly Detection Approach for Unmanned Aerial Vehicles. 2020 Int Wirel Commun Mob Comput IWCMC 2020 2020:469–74. 10.1109/IWCMC48107.2020.9148073.
[23] Ghalamchi Behnam, Jia Zheng, Mueller Mark Wilfried. Real-time vibration-based propeller fault diagnosis for multicopters. IEEE/ASME Trans Mechatronics 2020;25(1):395–405. https://doi.org/10.1109/TMECH.351610.1109/TMECH.2019.2947250.
[24] Kantue P, Pedro JO. Integrated Fault Detection and Diagnosis of an Unmanned Aerial Vehicle using Time Difference of Arrival 2020:336–42. 10.1109/icstcc50638.2020.9259777.
[25] Ray DK, Roy T, Chattopadhyay S. Skewness Scanning for Diagnosis of a Small Inter-Turn Fault in Quadcopter's Motor based on Motor Current Signature analysis. IEEE Sens J 2020;XX:1–1. 10.1109/jsen.2020.3038786.
[26] Keipour A, Mousaei M, Scherer S. Automatic real-time anomaly detection for autonomous aerial vehicles. ArXiv 2019:5679–85.
[27] Wang X, Fan W, Li X, Wang L. Weak degradation characteristics analysis of UAV motors based on laplacian eigenmaps and variational mode decomposition. Sensors (Switzerland) 2019;19. 10.3390/s19030524.
[28] Pourpanah F, Zhang B, Ma R, Hao Q. Anomaly Detection and Condition Monitoring of UAV Motors and Propellers. Proc IEEE Sensors 2018;2018-Octob:2018–21. 10.1109/ICSENS.2018.8589572.
[29] Aboutalebi Payam, Abbaspour Alireza, Forouzannezhad Parisa, Sargolzaei Arman. A novel sensor fault detection in an unmanned quadrotor based on adaptive neural observer. J Intell Robot Syst Theory Appl 2018;90(3-4):473–84. https://doi.org/10.1007/s10846-017-0690-7.
[30] Ferrão IG, Pigatto DF, Fontes JVC, Silva NBF, Espes D, Dezan C, et al. STUART: ReSilient archiTecture to dynamically manage Unmanned aeriAl vehicle networks under atTack. Proc - IEEE Symp Comput Commun 2020;2020-July. 10.1109/ISCC50000.2020.9219689.
[31] Johry A, Kapoor M. Unmanned aerial vehicle (UAV): fault tolerant design. Int J Eng Technol Sci Res IJETSR Wwwljetsrcom ISSN 2016;3:2394–3386.
[32] Awadallah MA, Morcos MM, Gopalakrishnan S, Nehl TW. A neuro-fuzzy approach to automatic diagnosis and location of stator inter-turn faults in CSI-fed PM brushless DC motors. IEEE Trans Energy Convers 2005;20(2):253–9. https://doi.org/10.1109/TEC.2005.847976.
[33] Sadeghzadeh I, Zhang Y. A review on fault-tolerant control for unmanned aerial vehicles (UAVs). AIAA Infotech Aerosp Conf Exhib 2011;2011:1–12. https://doi.org/10.2514/6.2011-1472.

[34] Yaman Orhan, Tuncer Turker, Tasar Beyda. DES-Pat: a novel DES pattern-based propeller recognition method using underwater acoustical sounds. Appl Acoust 2021;175:107859. https://doi.org/10.1016/j.apacoust.2020.107859.
[35] Yaman Orhan, Ertam Fatih, Tuncer Turker. Automated Parkinson's disease recognition based on statistical pooling method using acoustic features. Med Hypotheses 2020;135:109483. https://doi.org/10.1016/j.mehy.2019.109483.
[36] Park J-H, Jun C-Y, Jeong J-Y, Chang DE. Real-time quadrotor actuator fault detection and isolation using multivariate statistical analysis techniques with sensor measurements 2020:33–7. 10.23919/iccas50221.2020.9268391.